


Cite this: *RSC Adv.*, 2022, **12**, 8918

Carbohydrate structure–activity relations of Au-catalysed base-free oxidations: gold displaying a platinum lustre†

Frits van der Klis,^{ab} Linda Gootjes,^b Noud Hendrik Verstijnen,^b Jacco van Haveren,^b Daniël Stephan van Es^{ID *b} and Johannes Hendrik Bitter^{ID *a}

This paper describes the base-free gold-catalysed oxidation of four different carbohydrates in a packed bed plug flow reactor. The influence of the carbohydrate structure on the catalytic activity and selectivity was investigated by comparing two neutral sugars (glucose (Glc) and galactose (Gal), both with primary alcohols at C6), with their sugar-acid analogues (glucuronic acid (GlcA) and galacturonic acid (GalA), both with carboxylic acids at C6). The orientation of OH-groups at the C4-position (*equatorial* in Glc/GlcA and *axial* in Glc/GlcA), and the C6-functionality (primary alcohols in Gal/Glc and carboxylic acids in GalA/GlcA) has a profound influence on the catalytic activity. When the OH-groups are in an *axial* position their reactivity was higher compared to the OH-groups in the *equatorial* position for both the sugars and the sugar acids. In addition the reactivity of carbohydrates over Au-catalysts under base-free conditions is different compared to alkaline conditions, and is more in line with a Pt-catalysed dehydrogenation mechanism.

Received 13th January 2022

Accepted 14th March 2022

DOI: 10.1039/d2ra00255h

rsc.li/rsc-advances

1. Introduction

Agricultural residues with low nutritional value are attractive feedstocks for the production of chemicals and materials, while not competing with food or land-use. These residues are generally rich in carbohydrates, and can be converted into useful chemicals¹ such as sugar acids and lactones *via* green catalytic oxidation reactions.² These sugar acids and lactones have already shown many potential applications, ranging from platform molecules for polymer building blocks (including FDCA), sequestering agents, corrosion inhibitors, food additives, and many more.^{3–5}

Over the past decades, supported gold nanoparticles have proven to be excellent catalysts for carbohydrate oxidations. Extensive research on the influence of particle size, catalyst support, preparation methods, as well as catalyst deactivation mechanisms, has contributed to in-depth understanding of the influence of the Au-catalyst morphology on the oxidation performance.^{6–14} Furthermore, reaction mechanisms have been proposed for both alkaline- and base-free conditions. Despite this great knowledge on Au-catalyst structure–activity

relationships, much less is known about the influence of carbohydrate structures on catalytic oxidation reactions at the gold surface.

To establish such a structure–activity relationship for carbohydrates, substituent variation of carbohydrates with otherwise identical conformations should be compared. Fig. 1 shows four (relevant and natural abundant) carbohydrates, organised in such a way that systematic comparison of only one

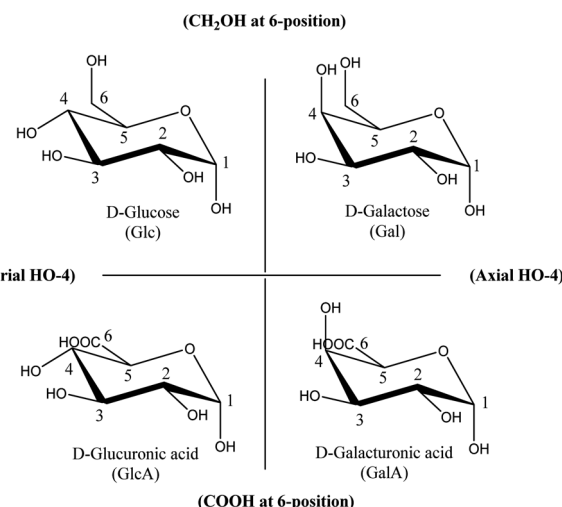


Fig. 1 Carbohydrate structures investigated in this paper, represented as α -D-pyranosides.

^aWageningen University Biobased Chemistry and Technology, Bornse Weilanden 9, 6708 WG, Wageningen, The Netherlands. E-mail: harry.bitter@wur.nl; Tel: +31 317 480 303

^bWageningen Food & Biobased Research, Bornse Weilanden 9, 6708 WG, Wageningen, The Netherlands. E-mail: daan.vanes@wur.nl; Tel: +31 317 481 160

† Electronic supplementary information (ESI) available. See DOI: [10.1039/d2ra00255h](https://doi.org/10.1039/d2ra00255h)



substituent is possible over each axis. The horizontal axis shows sole variation in the orientation of the OH-group at the C4-position, while the vertical axis shows the variation in only the C6-position.

The influence of conformation of the four carbohydrate structures depicted in Fig. 1 on catalytic oxidations has been previously investigated for platinum catalysts: the pioneering work of De Wit *et al.*¹⁵ focussed on establishing carbohydrate oxidation rates (actually dehydrogenation rates) under strong alkaline conditions (1 M KOH) in the absence of oxygen over Pt- and Rh-catalysts.

The following influence on oxidation rate was found: for the HO-4 orientation *Axial* > *Equatorial*; and for the 6-position $\text{CH}_2\text{OH} > \text{CO}_2^-$. (Thus for the carbohydrates in Fig. 1: Gal > Glc > GalA > GlcA.) The higher reactivity of Gal compared to Glc, only differing in their HO-4 orientation, was later confirmed by others for Pt- and Pd-catalysts under milder reaction conditions (pH 9) and in the presence of oxygen.¹⁶

For Au-catalysts, comparable research on carbohydrate structure-activity relations was solely performed *under alkaline conditions* in the presence of oxygen. Surprisingly, Au behaves completely different compared to Pt under these alkaline conditions: *e.g.* Glc oxidation is much faster compared to Gal^{16,17} (*Equatorial* HO-4 preferred over *axial* orientation for Au, contrary to Pt). Rautiainen *et al.*¹⁸ included variation at C6 (CH_2OH and CO_2^-), by adding the uronic acid analogues GlcA and GalA, but did not find a large influence of C6-position on the reaction rate (Glc > Gal \approx GlcA \approx GalA), while De Wit *et al.*¹⁵ clearly found this influence for Pt-catalysts (Gal > Glc > GalA > GlcA). The ESI provides a complete overview of carbohydrate conformations (Table S1†) and previously reported oxidation rates (Table S2†).

The question what causes the observed differences in reactivity for gold compared to other metals like platinum and palladium was already raised in 2006 by Mirescu & Prüße:¹⁶

"The Au catalyst displayed the highest activity in glucose oxidation, whereas the same catalyst oxidized the galactose more slowly. It appears that the structure of the sugars influences the activity of the Au catalyst but not in the same manner as it does for Pt catalysts. A detailed mechanism of carbohydrates' oxidation on an Au catalyst has not yet been reported."

As we will show later in this paper, Au-catalysts under base-free conditions do resemble the performance of Pt catalysts. Therefore we will focus on the mechanisms of Au oxidations in some more detail here as well. Despite today's knowledge on the oxidation mechanisms of Au-catalysts, to the best of our knowledge the question with regard to the reactivity differences between Pt and Au has not yet been answered. In the meantime, carbohydrate oxidations over Au-catalysts have evolved in two directions: besides the "classical" alkaline conditions, also base-free oxidations using Au have been developed.^{7,8,12,14,19-23} It is believed that Au-catalysed reactions under alkaline conditions follows a completely different reaction mechanism (Fig. 2A) compared to base-free conditions (Fig. 2B).

The alkaline mechanism is believed to proceed *via* an opening intermediate, while the base-free mechanism occurs *via* the adsorption of the anomeric OH functionality, thus with the

carbohydrate still in cyclic form. The base-free mechanism thereby closer resembles the Pt-dehydrogenation mechanism as proposed by De Wit *et al.*¹⁵ It is therefore to be expected that structural differences of the carbohydrates have a different impact, depending on the oxidation mechanism. In other words: for base-free oxidations a different influence of carbohydrate-structure on the reaction rates might be expected, than has been established for Au under alkaline conditions.

Our hypothesis is therefore that Au will behave like Pt under base-free conditions. Hence, the aim of this study is to establish a structure-activity relationship for Au-catalysed carbohydrate oxidations under base-free conditions by systematically comparing four structurally related carbohydrates under flow conditions in a fixed bed reactor over gold on titania.

2. Experimental

2.1 Materials and chemicals

2.1.1 Chemicals used for catalytic oxidation reactions. Oxygen gas (4.5) was obtained from Linde Gas, The Netherlands. Granular Au/TiO₂ was obtained from Strem (gold on titania, Aurolite™ 1.2 wt% Au/TiO₂, AuTEK). The BET surface area of this catalyst is $47 \text{ m}^2 \text{ g}^{-1}$, with an average Au-particle size of 2.5 nm (determined by TEM and STEM).²⁵ The reported Au-loading of 1.1–1.2 wt% was confirmed by ICP measurements.^{25,26} XRD measurements showed that the titania support is of the mixed anatase/rutile-type. The pH of our reaction mixtures is acidic in nature (pH 1.5–2 after reaction), and therefore below the points of zero charge of both rutile and anatase.²⁷ As a result the support will be positively charged under the applied reaction conditions. Previously investigations showed that the TiO₂-support itself is not active in the conversion of the substrates.^{25,28} This granular Au/TiO₂-catalyst was gently crushed and sieved to obtain an equal particle size of 0.5–0.65 mm for experiments in plug flow set-up. Silicon carbide (powder, medium, 120 grit, Alfa Aesar) was used as additional inert filler for the packed bed plug flow reactor. The following carbohydrate substrates were used as received: alpha-D-glucose (96%, Sigma Aldrich), D-(+)-galactose (99+, Acros), D-glucuronic acid (>96.0%, TCI), D-galacturonic acid monohydrate (gift from Royal Cosun).

2.1.2 Chemicals used as analytical standards. For analytical standards (HPLC analysis) the following chemicals were used as received: calcium saccharate tetrahydrate (98–102%, Sigma Aldrich); galactaric acid (mucic acid; 97%, Sigma-Aldrich); D-galactonic acid, calcium salt (Aldrich); D-galactose (99%, Sigma Aldrich); D-galacturonic acid sodium salt (purum, Sigma-Aldrich); D-(+)-gluconic acid sodium salt (>99%, Merck); D-(+)-gluconic acid δ -lactone (99.0%, Sigma Aldrich); D-(+)-glucose (>99.5% GC, VWR); D-saccharic acid-1,4-lactone monohydrate (>98% HPLC, Merck). Sulfuric acid (95–97%, for analysis, Merck) was used to prepare the HPLC eluent. Additional reference compounds were synthesized in-house (see under Sections 2.1.3 and 2.4).

2.1.3 Chemicals used for reference compound synthesis. The following chemicals and solvents were used without further purification: acetic acid (>99%, VWR Chemicals); acetone



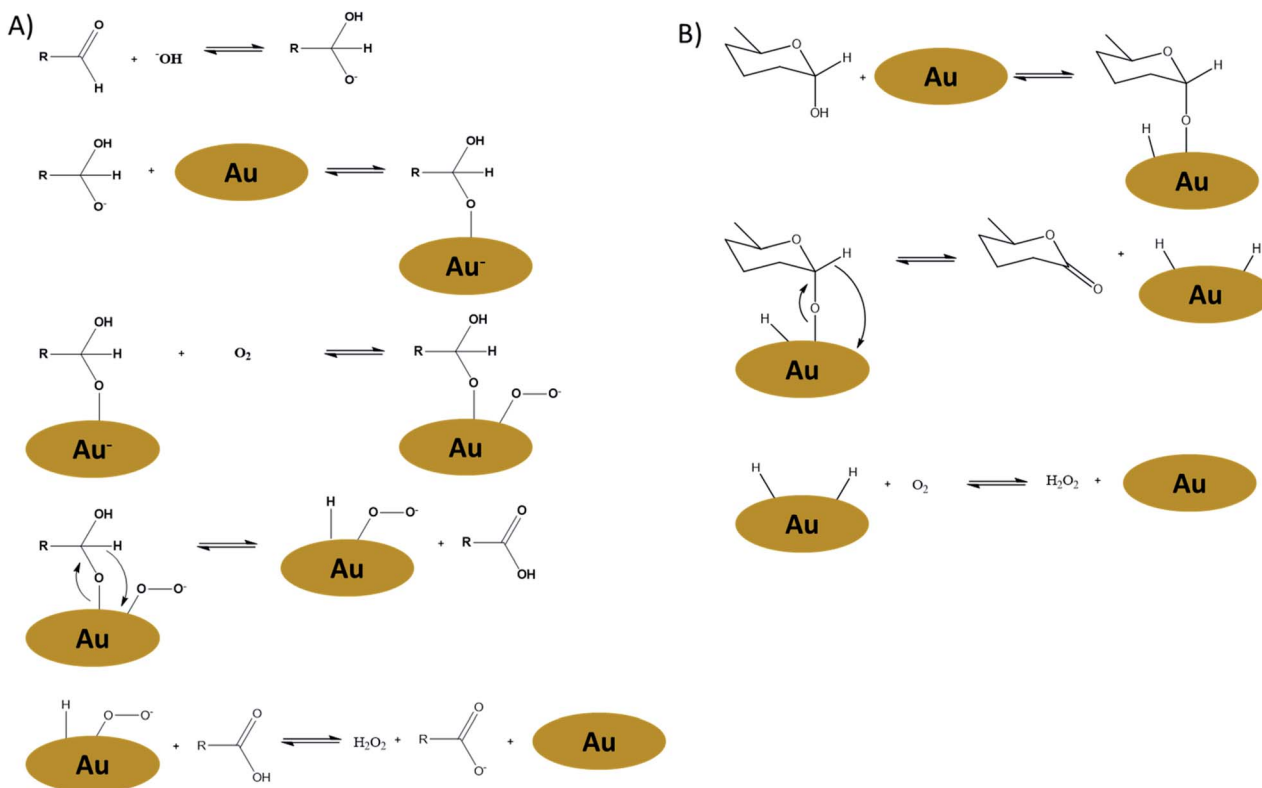


Fig. 2 (A) Proposed reaction mechanism for Au-catalysed alkaline oxidation of carbohydrates in the presence of oxygen,²⁴ and (B) proposed reaction mechanism for Au-catalysed base-free oxidation of carbohydrates in the presence of oxygen.²²

(≥99%, VWR Chemicals); Amberlite® IR-120 hydrogen form (IE-resin, Fluka analytical); bromine (≥99%, Alfa Aesar); BSTFA + TMCS (99 : 1, silylation reagent, Supelco); Celite® (Alfa Aesar); D-(+)-gluconic acid δ -lactone (≥99.0%, Sigma Aldrich); D-galactose (≥99%, Sigma Aldrich); D-galacturonic acid monohydrate (batch C-9, gift by Royal Cosun); diethyl ether (≥99.5%, Actu-All chemicals); absolute ethanol (100%, VWR Chemicals); ethyl acetate (≥99.7%, Honeywell); hydrochloric acid (37%, VWR Chemicals); magnesium sulfate (Alfa Aesar); mucic acid (≥97%, Sigma Aldrich); potassium carbonate (≥99.5%, Merck); pyridine (≥99.5%, Merck); Sicapent® (Merck Millipore); sodium bicarbonate (≥99.5%, Merck); sodium bisulfite (Acros Organics); sodium hydroxide (2 M standard solution, Fluka analytical); sodium thiosulfate (≥98%, Sigma Aldrich); sulfuric acid (95–97%, Sigma Aldrich).

2.2 Protocol for carbohydrate oxidation reactions in the packed bed plug flow reactor

All catalytic oxidation reactions were performed in a packed bed plug flow reactor set-up as described in detail previously.²⁶ The catalyst bed of the packed bed reactor was filled with 1 wt% Au/TiO₂ (7.7 g; crushed and sieved), and the catalyst particles were mixed with additional inert silicon carbide powder to fill the voids. For each reaction, the desired temperature was set (variation between 40–100 °C), and 0.1 M aqueous solutions of the carbohydrates were fed to the reactor at a flow rate of 10 mL min⁻¹. Oxygen gas was applied at a flow rate of 50 mL min⁻¹, and the total system pressure was kept constant at

10 bar. The contact time of the reactants with the catalyst bed was approximately 1.3 min.

All oxidation reactions were performed using the above described set-up and conditions, and the following protocol to determine the conversion of the carbohydrates was applied: reactions were initiated by applying the fixed oxygen- and liquid flows at a system pressure of 10 bar, and the desired temperature was set. Next, the reactor was allowed to stabilize for 1 h. During this time no samples were collected, to allow the system to stabilise. After one hour, sample collection was started at time intervals of 10 min. For a period of 1 h (total reaction time including stabilisation is therefore 2 h per setting). As a sample was collected each 10 min, during 1 h collection time, for each condition a total of five samples was obtained.

The collected liquid samples were stored at 4 °C for analysis by HPLC, and/or colorimetric methods to determine the conversion and product composition. Additionally, some samples were subjected to crash freezing immediately after they left the reactor, followed by lyophilizing, to obtain dry samples for additional NMR analysis (Section 1 of ESI†).

Section 1 of the ESI† also provides a comparison to the appropriate reference compounds (see under 2.4) as well as an in-depth discussion on potential pathways and kinetics.

2.3 Analytical equipment

2.3.1 HPLC analysis and colorimetric method. HPLC analyses were performed on a Waters e2695 HPLC instrument, equipped with a Concise Corogel Ion 300 (30 cm length)



column, maintained at 65 °C, using H_2SO_4 (3 mM) in MilliQ water as the eluent, with a flow rate of 0.4 mL min⁻¹. The components were identified using a Waters 2489 UV/Vis Detector (210 nm) and a Waters 2414 RI detector. An overview of all retention times (both RI and UV) is provided in Table S3 of the ESI,† and the HPLC spectra are displayed in ESI Fig. S48–S61.†

As the conversion of GlcA could not be determined by HPLC due to overlapping peaks, a colorimetric method described as the “TTC-Protocol” in Botelho da Silva *et al.*²⁹ & Jaušovec *et al.*³⁰ was used to determine the conversion for the GlcA reactions.

2.3.2 GC-MS. Analyses were performed using an Interscience TraceGC Ultra GC with an AS3000 II auto sampler. Products were separated over a Restek GC column (Rxi-5ms 30 m × 0.25 mm × 0.25 μm). Helium was used as the carrier gas, with a flow of 1 mL min⁻¹, and a split flow of 20 mL min⁻¹. Temperature program: hold 3 min at 50 °C, ramp 7.5 °C min⁻¹, final temperature 330 °C. An Interscience TraceDSQ II XL quadrupole mass selective detector (EI, mass range 35–500 Dalton, 150 ms sample speed) was used for detection. Samples were silylated by dissolving 2–5 mg mL⁻¹ in pyridine (≥99.5%, Merck), and adding 100 μL BSTFA + TMCS (99 : 1, silylation reagent, Supelco) followed by storing the sample at 70 °C for 20 min. prior to analysis.

2.3.3 NMR. Spectra were recorded on a Bruker Avance III spectrometer operating at 400.17 MHz (¹H) and 100.62 MHz (¹³C) in DMSO-D6 (99.5 atom % D, contains 0.03% v/v TMS, Sigma Aldrich). Chemical shifts are quoted in parts per million (ppm) referenced to DMSO-D6.

2.3.4 FTIR. Spectra were obtained on a Varian Scimitar 1000 FTIR spectrometer equipped with a Pike MIRacle ATR Diamond/ZnSe single reflection plate and a DTSG-detector. The measurement resolution was set at 4 cm⁻¹, and the spectra were collected in the range 4000–650 cm⁻¹ with 64 co-added scans.

2.3.5 Melting point. Melting points were measured on a Thermo Scientific 9200 melting point apparatus. The temperature ramp was set at 1 °C min⁻¹.

2.4 Synthesis of lactone references and detailed analysis of oxidation reaction mixtures

All potential lactone products, resulting from the catalytic oxidation reactions in Section 2.2, which were not commercially available were synthesized in-house. A detailed description of their synthesis and analysis can be found in Section 2 of the ESI.†

3. Results and discussion

The structural influence of four common carbohydrates (Fig. 1) on their catalytic oxidation over Au/TiO₂ under base-free conditions was investigated: D-glucose and D-galactose (differing only in HO-4 orientation) and their related uronic acid derivatives D-glucuronic acid and D-galacturonic acid (also differing in C-6 functionality).

All conversions were performed without added base, so under initial neutral conditions for Glc and Gal, and under the

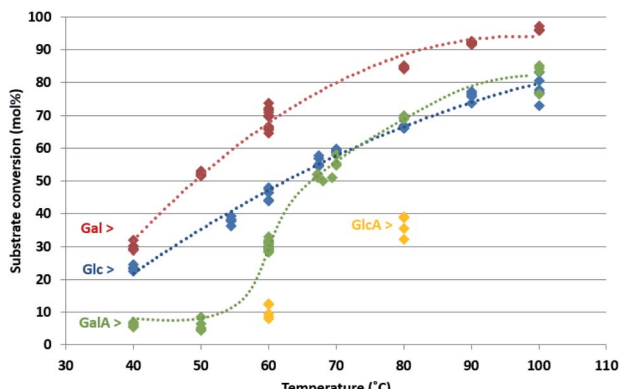


Fig. 3 Substrate conversion as a function of reaction temperature; Gal (red), Glc (blue), GalA (green) and GlcA (yellow). Dots represent experimental data points, the dotted lines are added as a visual reference to guide the eye over the general conversion trends. Reaction conditions: Au/TiO₂ catalyst, substrate concentration = 0.1 M (10 mL min⁻¹), oxygen (10 bar pressure, 50 mL min⁻¹).

natural pH (acidic) for GlcA and GalA. The conversions were investigated over a temperature range from 40–100 °C. The number of temperature variations performed with D-glucuronic acid was limited due to the relative high price of this substrate, and the high amounts needed in our experimental set-up.

Fig. 3 shows the conversion of the four carbohydrates as a function of reaction temperature. The diamond shapes represent the individual HPLC/colorimetric measurement points of the obtained samples (for each reaction temperature and carbohydrate, five individual measurements were obtained). The dotted lines are added as a visual reference to guide the eye over the conversion trend as a function of temperature. A similar graph, which expresses the same data as substrate conversion rates, is included in the ESI, Fig. S7.†

As can be seen from the graph in Fig. 3, the conversion of the carbohydrates was stable over the course of the reactions, resulting in a low spread (≤5% experimental error) in conversion.

The influence of the HO-4 orientation on the conversion can be found by comparing the two neutral sugars: over the whole temperature range, 40–100 °C, the conversion of Gal was higher compared to Glc. This indicates that for the neutral sugars (CH₂OH at C6) the *axial* HO-4 orientation in Gal is preferred over the *equatorial* HO-4 orientation in Glc. A same preference was found for their acidic analogues with COOH at C6: the *axial* HO-4 orientation in GalA leads to higher reactivity compared to the *equatorial* HO-4 orientation in GlcA. The rate promoting effect of the *axial* HO-4 orientation is thus universal in both the neutral- and acidic sugars.

The influence of the C6 position is shown by the higher conversion of Glc (CH₂OH at C6), compared to the lower conversion of its acidic analogue GlcA (COOH at C6). An identical effect is found for the galacto-series: Gal (CH₂OH at C6) shows higher conversions compared to the sugar acid analogue GalA (COOH at C6) over the whole temperature range (40–100 °C). This result indicates a clear rate deteriorating effect of the carboxylic acid functionality compared to the primary OH at C6.



At temperatures between 40 and 60 °C, the reactivity of Glc is higher compared to GalA, while at temperatures above 60 °C the reactivity's are almost identical. This indicates that the extent of the reactivity promoting effect of *axial* HO-4 orientation, and the reactivity decreasing effect of a carboxylate group at C6, have different influence on the activation energy: a stronger effect of the carboxylic acid functionality compared to the effect of the HO-4 position. It is generally accepted that pH plays an important role during Au-catalysed oxidation reactions. The lowered reactivity of the acidic sugars compared to the neutral sugars might be caused by this effect. However, it should be realized that lactones and sugar acids are formed as products during reaction. We found that the pH of all reaction mixtures was between pH 1.5–2 when they left the reactor, indicating that there is not much variation in pH of the final product mixtures.

To summarize, the following effect of the carbohydrate structure on the reaction rate has been established: Gal > Glc > GalA > GlcA. These results, we have obtained in this study under base-free conditions, differs from the results previously observed by others for Au-catalysts under alkaline conditions: Glc > Gal \approx GlcA \approx GalA,¹⁸ but is an exact match with the previous findings for Pt-catalysts.¹⁵ This is a first confirmation of the hypothesis that Au under base-free conditions is acting in a similar way as Pt.

To gain more insight in the mechanism occurring during base-free carbohydrate oxidation, conformation of lactone formation during the reactions was needed. Therefore the presence of lactones in the reaction mixtures was investigated by taking samples of the reaction mixtures directly after they left the reactor, followed by immediate crash-freezing of the samples. Next, samples were lyophilized, and analysed by NMR in DMSO-*D*₆. DMSO was chosen as the solvent, to avoid potential ring opening of lactones in D₂O during the measurements. All obtained spectra can be found in Section 1 of the ESI.†

The samples of the reaction mixtures for Glc, Gal and GalA were compared to the NMR spectra of the starting materials, all potential lactone products (1,4- and 1,5-lactones), as well as the sugar acids in open form. In case reference samples were not commercially available, the lactones were synthesized *via* independent synthesis methods. An elaborate description of the synthesis of the reference lactones as well as their analysis is described in Section 2 of the ESI.†

For all investigated carbohydrate oxidation reactions, the presence of lactones in the freeze dried samples was confirmed: GalA oxidation resulted in a mixture of remaining starting material, galactaric acid-1,4-lactone, and galactaric acid (di-acid in open form); consult ESI, Sections 1.1 & 1.2.† For Gal, a very similar product mixture was found: Unreacted starting material, galactonic acid-1,4-lactone and galactonic acid in open form; consult ESI, Section 1.4.† For Glc, next to starting material and gluconic acid in open form, both the gluconic acid-1,4-lactone and gluconic acid-1,5-lactone were found; consult ESI, Section 1.3.† The synthesis of the reference compounds, the analysis results of the free-dried reaction mixtures, and an in-depth discussion on the obtained results can be found in the ESI.†

To summarize, the detailed product analysis which clearly indicated the formation of lactone products, is another

indication that the mechanism of Au-catalysed oxidations under base-free conditions resembles a Pt-like oxidation (dehydrogenation) mechanism.

4 Conclusions

The base-free catalytic oxidation of four different carbohydrates over Au/TiO₂ was investigated in a plug flow packed bed reactor set-up over a range of different temperatures, aiming to establish a structure–activity relationship.

It was found that the reactivity of D-galactose (*axial* HO-group in 4-position) was higher compared to D-glucose (*equatorial* HO-group in 4-position) over the temperature range investigated (40–100 °C). The same influence of the HO-4 position was found by the higher reactivity of D-galacturonic acid (*axial* HO-group in 4-position) compared to D-glucuronic acid (*equatorial* HO-group in 4-position). The reactivity of the two uronic acids, galacturonic acid and glucuronic acid, which both have an carboxyl moiety at C6, is lower compared to their aldose analogues, both with primary CH₂OH moieties at C6. This indicates a rate-deteriorating effect of carboxyl groups at C6 over primary alcohols at C6.

At temperatures between 40 and 60 °C, the reactivity of glucose is higher compared to galacturonic acid, while at temperatures above 60 °C the reactivity's are almost identical. This indicates that the extent of the reactivity promoting effect of *axial* HO-4 orientation, and the reactivity decreasing effect of a carboxylate group at C6, are both temperature dependant.

Our study has shown that the structure–activity relationship of carbohydrate oxidations over an Au-catalyst under base-free conditions is completely different from those under alkaline conditions. We tentatively attribute this to a difference between these two reaction mechanisms: under alkaline conditions the carbohydrates orientate in open form to the catalyst surface, while under acidic conditions the oxidation proceeds *via* adsorption of the carbohydrate in a closed ring conformation. This results in different interaction with the catalyst surface, thereby resulting in a different preference for the orientation of substituents interacting with this gold surface. Our hypothesis was that the Au-catalysed mechanism resembles a platinum-like hydrogen abstraction mechanism, and should therefore follow the same structure–activity relationship. This has now been confirmed for the first time, by showing that Au-catalysts under base-free conditions indeed resemble the results of Pt-catalysts. The results obtained in this study pave the way for further (computational) investigations, to elucidate the exact interaction of the carbohydrates with the catalyst surface.

Conflicts of interest

There are no conflicts to declare.

Acknowledgements

This research is part of a project that has received funding from the Bio Based Industries Joint Undertaking under the European Union's Horizon 2020 research and innovation programme



under grant agreement No 669105. The authors would like to thank David Franciolus for assisting with the HPLC analysis, Guus Frissen for NMR measurements, and Royal Cosun for supplying galacturonic acid.

Notes and references

- 1 R. A. Sheldon, *Curr. Opin. Green Sustain. Chem.*, 2018, **14**, 89–95.
- 2 L. T. Mika, E. Cséfalvay and Á. Németh, *Chem. Rev.*, 2018, **118**, 505–613.
- 3 R. M. de Lederkremer and C. Marino, *Adv. Carbohydr. Chem. Biochem.*, 2003, **58**, 199–306.
- 4 T. Mehtio, M. Toivari, M. G. Wiebe, A. Harlin, M. Penttilä and A. Koivula, *Crit. Rev. Biotechnol.*, 2016, **36**, 904–916.
- 5 N. M. Xavier, A. P. Rauter and Y. Queneau, *Top. Curr. Chem.*, 2010, **295**, 19–62.
- 6 M. Sankar, Q. He, R. V. Engel, M. A. Sainna, A. J. Logsdail, A. Roldan, D. J. Willock, N. Agarwal, C. J. Kiely and G. J. Hutchings, *Chem. Rev.*, 2020, **120**, 3890–3938.
- 7 C. Megías-Sayago, L. F. Bobadilla, S. Ivanova, A. Penkova, M. A. Centeno and J. A. Odriozola, *Catal. Today*, 2018, **301**, 72–77.
- 8 C. Megías-Sayago, J. L. Santos, F. Ammari, M. Chenouf, S. Ivanova, M. A. Centeno and J. A. Odriozola, *Catal. Today*, 2018, **306**, 183–190.
- 9 Y. Önal, S. Schimpf and P. Claus, *J. Catal.*, 2004, **223**, 122–133.
- 10 S. Porsgaard, P. Jiang, F. Borondics, S. Wendt, Z. Liu, H. Bluhm, F. Besenbacher and M. Salmeron, *Angew. Chem., Int. Ed.*, 2011, **50**, 2266–2269.
- 11 U. Prüsse, M. Herrmann, C. Baatz and N. Decker, *Appl. Catal. A*, 2011, **406**, 89–93.
- 12 P. Qi, S. Chen, J. Chen, J. Zheng, X. Zheng and Y. Yuan, *ACS Catal.*, 2015, **5**, 2659–2670.
- 13 F. Vigneron and V. Caps, *C. R. Chim.*, 2016, **19**, 192–198.
- 14 Y. Wang, S. Van de Vyver, K. K. Sharma and Y. Roman-Leshkov, *Green Chem.*, 2014, **16**, 719–726.
- 15 G. de Wit, J. J. de Vlieger, A. C. Kock-van Dalen, R. Heus, R. Laroy, A. J. van Hengstum, A. P. G. Kieboom and H. van Bekkum, *Carbohydr. Res.*, 1981, **91**, 125–138.
- 16 A. Mirescu and U. Prüsse, *Appl. Catal., B*, 2007, **70**, 644–652.
- 17 U. Prüsse, K. Heidkamp, N. Decker, M. Herrmann and K. D. Vorlop, *Chem. Ing. Tech.*, 2010, **82**, 1231–1237.
- 18 S. Rautiainen, P. Lehtinen, J. Chen, M. Vehkamaki, K. Niemela, M. Leskela and T. Repo, *RSC Adv.*, 2015, **5**, 19502–19507.
- 19 D. An, A. Ye, W. Deng, Q. Zhang and Y. Wang, *Chem. - Eur. J.*, 2012, **18**, 2938–2947.
- 20 Y. Cao, X. Liu, S. Iqbal, P. J. Miedziak, J. K. Edwards, R. D. Armstrong, D. J. Morgan, J. Wang and G. J. Hutchings, *Catal. Sci. Technol.*, 2016, **6**, 107–117.
- 21 M. Comotti, C. D. Pina and M. Rossi, *J. Mol. Catal. A: Chem.*, 2006, **251**, 89–92.
- 22 B. T. Kusema, J.-P. Mikkola and D. Y. Murzin, *Catal. Sci. Technol.*, 2012, **2**, 423–431.
- 23 P. J. Miedziak, H. Alshammari, S. A. Kondrat, T. J. Clarke, T. E. Davies, M. Morad, D. J. Morgan, D. J. Willock, D. W. Knight, S. H. Taylor and G. J. Hutchings, *Green Chem.*, 2014, **16**, 3132–3141.
- 24 U. Prüsse, S. Heidinger and C. Baatz, *Agric. Res.*, 2011, **3**, 261–272.
- 25 R. K. Pazhavelikkath Purushothaman, F. van der Klis, A. E. Frissen, J. van Haveren, A. Mayoral, A. van der Bent and D. S. van Es, *Green Chem.*, 2018, **20**, 2763–2774.
- 26 F. van der Klis, L. Gootjes, J. van Haveren, D. S. van Es and J. H. Bitter, *React. Chem. Eng.*, 2018, **3**, 540–549.
- 27 M. Kosmulski, *Adv. Colloid Interface Sci.*, 2002, **99**, 255–264.
- 28 J. Sha, *Bimetallic catalysts for oxidation of carbohydrates: looking for synergistic effects*, Ecole Centrale de Lille, 2018.
- 29 S. Botelho da Silva, M. Krolicka, L. A. M. van den Broek, A. E. Frissen and C. G. Boeriu, *Carbohydr. Polym.*, 2018, **186**, 299–309.
- 30 D. Jaušovec, R. Vogrinčič and V. Kokol, *Carbohydr. Polym.*, 2015, **116**, 74–85.

